Surface Quantum Dynamics

DOI: 10.1002/ange.201208868

Quantum Influences in the Diffusive Motion of Pyrrole on Cu(111)**

Barbara A. J. Lechner, Holly Hedgeland, John Ellis, William Allison, Marco Sacchi, Stephen J. Jenkins, and B. J. Hinch*

The adsorption of aromatic molecules on surfaces is of broad interest in the fields of self-assembled networks and self-organized growth.[1,2] During self-assembly, adsorbates diffuse and adjust their orientation to form regular superstructures. The result is a delicate balance between supramolecular chemistry (dipole–dipole interactions, hydrogen bonding, and van der Waals forces) and molecule–surface interactions. These factors determine the structure, energy, site-specificity, and two-dimensional molecular translational and rotational diffusion.[2–5] Differently substituted polyaromatic rings form key building blocks,[6] defining the structure of chemically functionalized surfaces. It is crucial to understand the motion of single molecular precursors to gain insight into the complex processes underlying self-assembly. Aromatic adsorbates are extended particles of large mass that are assumed to obey classical mechanics for temperatures where self-assembly occurs. We will see, however, that quantum effects can nevertheless play a crucial role in the dynamics of surface diffusion even when the quantized degrees of freedom are not associated directly with translational motion.

Here, we study pyrrole, C_4H_4NH, an important precursor for many chemically and technologically relevant materials. In recent years, functionalized pyrroles and related molecules have attracted increasing attention as self-assembling adsorbates.[7] Pyrrole has been studied on several metal surfaces, including Pt(111),[8] Pd(111),[9] Rh(111),[10] and Cu(100).[11] Whilst little is known about potential energy landscapes and interactions between molecules, pyrrole is usually found to adsorb in a flat-lying geometry at low coverages, often moving to a tilted geometry at higher coverages.

Herein we describe a helium spin-echo (HeSE) and density functional theory (DFT) study of the dynamics of this elementary building block on Cu(111) to investigate inter-adsorbate interactions, the effect of friction, and the role of quantum modes in a sub-monolayer regime. We will show that the behavior is dominated by the quantum contribution to the total energy of pyrrole's vibrational ground state. Surprisingly, the important vibrations are not those associated with motion of the center of mass but are internal modes.

The HeSE method is new and uniquely sensitive to atomic scale motion on pico- to nanosecond timescales.[12] Figure 1 illustrates the principle, showing how surface motion occurring over a time difference, t_{SE}, reduces coherent scattering and gives a correlation function that typically decays with time as $f(t) = a\exp(-\alpha t_{SE}) + c$.[12] The characteristic timescale of the motion is then given by the decay rate, α, which depends on the angle of scattering. Motion, in real space, is deduced by comparing the dependence on scattering angle, expressed as a momentum transfer, $\Delta\boldsymbol{K}$, with Langevin molecular dynamics (MD) simulations.[13]

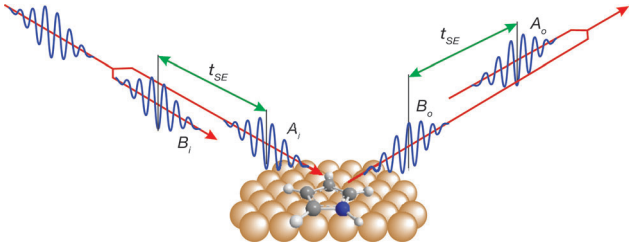

Figure 1. Schematic diagram of the HeSE experiment. The incident wavepacket is split and the two components, A_i and B_i, are separated so that they interrogate the surface with a time difference, t_{SE}. The lateral displacement of the components is shown for illustrative purposes only. The outgoing waves differ as a result of any motion occurring on the surface during t_{SE}. In this example, the outgoing component, A_o, is unchanged while B_o is phase-shifted by π. When the outgoing components are recombined the interference measures the de-coherence, which can be studied as a function of t_{SE}.

We have performed experiments at (121–170) K along two crystal directions. The resulting $\alpha(\Delta\boldsymbol{K})$ dependence is presented as data points in Figure 2a. The low $\Delta\boldsymbol{K}$ region is magnified in the inset for three coverages and a clear peak-and-dip feature can be seen to grow in intensity and move to larger $\Delta\boldsymbol{K}$ values with increasing coverage. The behavior indicates repulsive interactions giving rise to a quasi-hexagonal arrangement.[12] The position of the dips gives the coverage as 0.020, 0.033, and 0.052 monolayers (ML), respectively,[12] where one ML is defined as one adsorbate molecule per substrate atom. Comparing the results in Figure 2a with analytical models for diffusion, we rule out continuous Brownian motion which would give a quadratic relationship, leaving hopping motion as the most likely model for diffusion.[12] Hopping between sites forming a Bravais lattice is known to give zero decay at the diffraction

[*] Dr. B. A. J. Lechner, Dr. H. Hedgeland, Dr. J. Ellis, Dr. W. Allison
Cavendish Laboratory, University of Cambridge
J.J. Thomson Avenue, Cambridge, CB3 0HE (UK)
E-mail: bajl2@cam.ac.uk
Dr. M. Sacchi, Dr. S. J. Jenkins
Department of Chemistry, University of Cambridge
Lensfield Road, Cambridge, CB2 1EW (UK)
Prof. B. J. Hinch
Department of Chemistry and Chemical Biology, Rutgers University
Piscataway, NJ 08854 (USA)

[**] Financial support from the Austrian Academy of Sciences (B.A.J.L.), EPSRC (EP/E004962/1 H.H., J.E., W.A.; EP/J001643/1 M.S., S.J.J.) and the NSF (CHE 1124879 B.J.H.) is gratefully acknowledged.

Supporting information for this article is available on the WWW under http://dx.doi.org/10.1002/anie.201208868.

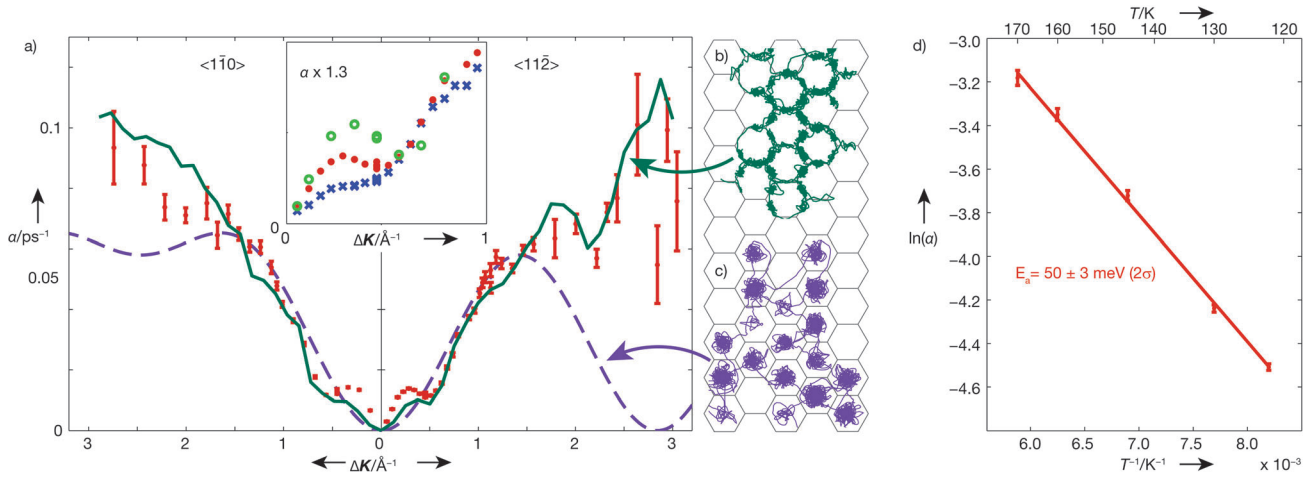

Figure 2. Experimental $\alpha(\Delta \boldsymbol{K})$ dependence for pyrrole/Cu(111) at 160 K compared to MD simulations. a) HeSE data for 0.033 ML coverage (points) compared to MD simulations for diffusion on bridge sites (solid line) and to predictions (see the Supporting Information) for single jumps on a simple Bravais lattice (dashed line). Corresponding adsorbate trajectories are illustrated in (b) and (c), respectively. The inset in (a) displays the coverage dependence in the low $\Delta \boldsymbol{K}$ region, caused by repulsive adsorbate interactions, for 0.020 (crosses), 0.033 (dots), and 0.052 ML coverage (circles). d) Arrhenius measurements for 0.033 ML pyrrole/Cu(111) at 0.9 $Å^{-1}$.

condition,[12] 2.84 $Å^{-1}$ along $\langle 11\bar{2} \rangle$ (dashed line in Figure 2a), which we do not observe. Hence, experiment suggests that pyrrole hops between bridge and/or hollow sites, not top sites.

DFT calculations show that pyrrole adsorbs in a flat-lying geometry on Cu(111), at a distance of 3 Å from the surface, analogous to the experimental observation for adsorption on other metal surfaces.[9–11] By relating calculated isocharge surfaces to the surface potential[14] we find that pyrrole is a symmetric scattering center. We determine adsorption energies at two coverages, $(\sqrt{7}x\sqrt{7})R19.1°$ and $(2\sqrt{3}x2\sqrt{3})R30°$, for a range of high-symmetry sites. For both coverages, centering over bridge sites is energetically preferred, while top sites are least favorable. We find a transition state above fcc and hcp hollow sites, creating a 15 meV barrier between bridge sites. The binding energy is nearly independent of the molecular orientation, implying that pyrrole can rotate freely on Cu(111).

Both calculations and experiment indicate multiple adsorption sites within the unit cell, suggesting motion in channels around top sites as illustrated in Figure 2b. However, at 160 K the calculated activation energy (15 meV) would give Brownian motion, as seen in benzene/graphite.[15] In contrast, measurements in Figure 2d show activated motion with a rate-limiting barrier[12] of (50 ± 3) meV, significantly higher than the calculated values for classical motion. One source of activation, not present in the calculations of the classical barrier, lies in the variation of the zero point energy (ZPE) between adsorption sites. Since the ZPE often does not greatly influence relative DFT adsorption energies it is commonly neglected. Here, however, the difference in ZPE between bridge and fcc sites is 14 meV, doubling the energy barrier, while the ZPE difference between bridge and hcp sites is 28 meV, almost tripling it.

Figure 3 illustrates the corrugation in the channels of bridge and hollow sites. Theoretical barriers excluding ZPE (dashed-dotted line) are much lower than the effective barrier found experimentally (shaded area). Only when ZPE changes

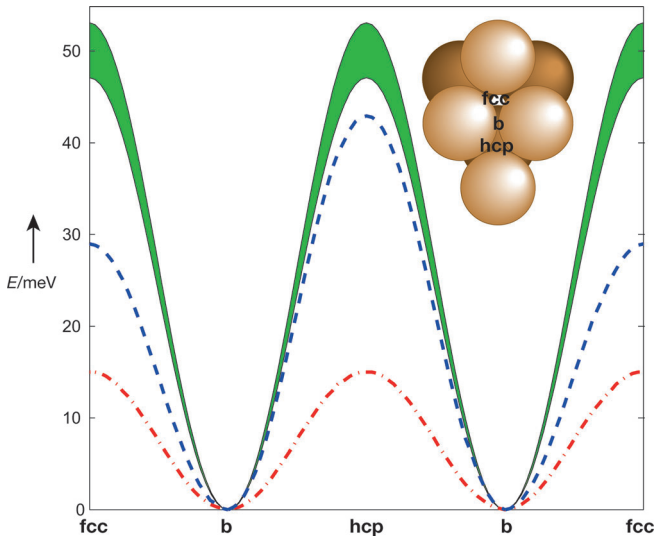

Figure 3. Pyrrole diffusion on Cu(111) is an activated process, as illustrated by the corrugation within channels of bridge and hollow sites. Standard DFT calculations (dashed-dotted line) show a small energy barrier. However, when ZPEs are included (dashed line), good agreement with the experimental rate-limiting barrier, indicated as the shaded area, is obtained. For illustrative purposes, values for adsorption sites have been connected by sinusoids.

are included (dashed line) does the calculated activation energy agree with experiment.[16] Note that the calculated barrier including ZPE is lower at the fcc site. The rate-limiting step for long-range diffusion, however, is determined by the largest barrier and the agreement between experiment and calculations is thus persuasive. We conclude that pyrrole adsorbs preferentially on bridge sites, moving over transition states above fcc and hcp sites. Figure 4 summarizes the relative contribution to the ZPE differences from key vibrational modes. The main contribution to the barrier stems from

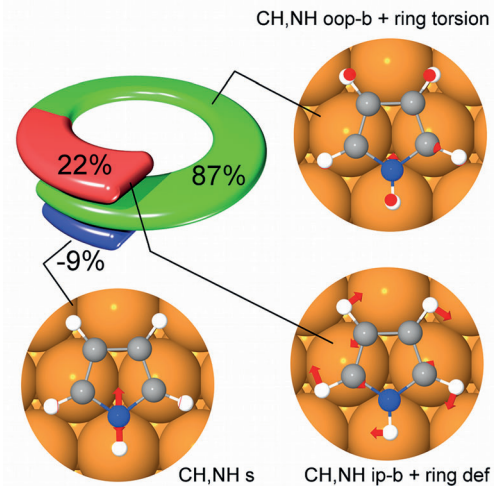

Figure 4. The contribution of key vibrational modes of pyrrole to the ZPE difference between the adsorption well and the transition state (hcp site), creating an increased activation barrier. At 87%, the largest contribution is made by the C–H and N–H out-of-plane bending (CH,NH oop-b) and ring torsion modes, while C–H and N–H in-plane bending (CH,NH ip-b) and ring deformation (ring def) modes account for the remaining 22%. The ZPEs of C–H and N–H stretching vibrations (CH,NH s) do not contribute significantly to the barrier (−9%), although they make the largest absolute contributions to the adsorption energy.

the C–H and N–H out-of-plane bending and ring torsion modes. This is interesting because the largest contributions to the absolute ZPE arise from C–H and N–H stretching modes, but these are more or less insensitive to the adsorption site.

By performing MD simulations,[13] modeling the motion of the center of mass over a two-dimensional potential energy surface (PES), we confirm that pyrrole hops between bridge sites, as shown in Figure 2. Excellent agreement with experiment is obtained, except in the region of very small $\Delta\boldsymbol{K}$ where the dipolar interactions in the MD simulations do not fully represent the complex interactions between adsorbate molecules. MD simulations provide a friction coefficient $\eta = 2.0\,ps^{-1}$ similar to that seen for benzene/graphite[15] and cyclopentadienyl/Cu(111).[3] At such high friction, pyrrole moves predominantly in single jumps between adjacent sites.

In summary, by combining experiment and theory we get a complete picture of the diffusion of pyrrole on Cu(111). The adsorbates move in single jumps between adjacent bridge sites over an apparent activation barrier of (50 ± 3) meV. Simulations reproduce the experimental results in a convincing manner. DFT calculations reveal that vibrational ZPEs provide much of the potential barrier for diffusion, even though the dominant modes are internal to the molecule and not frustrated translations. This behavior is thus phenomenologically different from the ZPE effects previously considered in quantum motion of hydrogenic adsorbates.[17] Our results show that purely quantum phenomena such as ZPEs can have a fundamental influence in the diffusion of even an aromatic molecule of large mass such as pyrrole. Whilst the effect may be less crucial when the activation barrier for total energy calculations is large, it clearly cannot be ignored in any system exhibiting weaker activation. In particular, we anticipate it to be of relevance to biochemical systems of large molecules exhibiting small barriers.

Experimental Section

A single-crystal Cu(111) sample (Surface Preparation Laboratory, Netherlands) was mounted inside an ultrahigh-vacuum chamber (background pressure: 2×10^{-11} mbar), and cleaned by Ar^+ sputtering (800 eV, 10 μA, 300 K) and annealing (800 K, 30 s). Surface cleanliness was checked using the helium reflectivity which was $\geq 35\%$ and the coverage controlled by monitoring the drop in reflectivity during uptake. Pyrrole (Sigma–Aldrich, reagent grade 98%) was purified by freeze–thaw cycles in high vacuum and dosed by backfilling the chamber. We find that pyrrole adsorbs reversibly below 200 K.

In Langevin MD simulations[13] the motion of a point particle was modeled as diffusion over a PES defined using the method described in the Supporting Information. We analyzed the lineshapes with a single exponential function, treating them in the same way as the experimental data. A barrier of 57 meV between bridge and hollow sites gave the best representation of the data and an activation energy of (49 ± 2) meV, in agreement with Figure 2d. Adsorbate–substrate interactions are included as a friction coefficient, η, and interadsorbate interactions are represented as pairwise dipoles using the calculated dipole moments.

DFT calculations were carried out within CASTEP.[18] Pyrrole/Cu(111) is a typical physisorbed system, where van der Waals forces predominate. Here we employed the dispersion force correction method developed in Ref. [19], where the Kohn–Sham energy of the system, calculated with the PBE functional, is corrected by adding a pairwise interatomic energy[20] and the C_6 coefficients are calculated from the ground-state electron density. The Cu(111) surface was modeled by a seven-layer slab where the top four layers are unconstrained. We used electronic and convergence parameters similar to those in Ref. [21]: 300 eV energy cut-off, a $(4 \times 4 \times 1)$ k-point grid, 0.05 e Å^{-1} force tolerance. The calculated total energies are given in the Supporting Information.

Received: November 5, 2012
Published online: March 26, 2013

Keywords: ab initio calculations · adsorption · single-molecule studies · surface chemistry · transition states

[1] S. Klyatskaya, F. Klappenberger, U. Schlickum, D. Kühne, M. Marschall, J. Reichert, R. Decker, W. Krenner, G. Zoppellaro, H. Brune, J. V. Barth, M. Ruben, *Adv. Funct. Mater.* **2011**, *21*, 1230–1240.
[2] J. V. Barth, G. Costantini, K. Kern, *Nature* **2005**, *437*, 671.
[3] H. Hedgeland, B. A. J. Lechner, F. E. Tuddenham, A. P. Jardine, W. Allison, J. Ellis, M. Sacchi, S. J. Jenkins, B. J. Hinch, *Phys. Rev. Lett.* **2011**, *106*, 186101.
[4] R. Gomer, *Rep. Prog. Phys.* **1990**, *53*, 917–1002.
[5] S. Paterson, W. Allison, H. Hedgeland, J. Ellis, A. P. Jardine, *Phys. Rev. Lett.* **2011**, *106*, 256101.
[6] a) S. Stepanow, R. Ohmann, F. Leroy, N. Lin, T. Strunskus, C. Wöll, K. Kern, *ACS Nano* **2010**, *4*, 1813–1820; b) J. A. A. W. Elemans, S. Lei, S. De Feyter, *Angew. Chem.* **2009**, *121*, 7434–7469; *Angew. Chem. Int. Ed.* **2009**, *48*, 7298–7332.
[7] a) S. Park, J.-H. Lim, S.-W. Chung, C. A. Mirkin, *Science* **2004**, *303*, 348; b) Y.-C. Liu, S.-J. Yang, T. C. Chuang, C.-C. Wang, *J. Electroanal. Chem.* **2004**, *570*, 1–5.
[8] G. Tourillon, S. Raaen, T. A. Skotheim, M. Sagurton, R. Garrett, G. P. Williams, *Surf. Sci.* **1987**, *184*, L345–L354.
[9] a) C. J. Baddeley, C. Hardacre, R. M. Ormerod, R. M. Lambert, *Surf. Sci.* **1996**, *369*, 1; b) D. N. Futaba, S. Chiang, *J. Vac. Sci.*

Technol. A **1997**, *15*, 1295; c) T. E. Caldwell, D. P. Land, *Polyhedron* **1997**, *16*, 3197.
[10] F. P. Netzer, E. Bertel, A. Goldmann, *Surf. Sci.* **1988**, *199*, 87.
[11] B. A. Sexton, *Surf. Sci.* **1985**, *163*, 99 – 113.
[12] A. P. Jardine, H. Hedgeland, G. Alexandrowicz, W. Allison, J. Ellis, *Prog. Surf. Sci.* **2009**, *84*, 323.
[13] G. Alexandrowicz, P. R. Kole, E. Y. M. Lee, H. Hedgeland, R. Ferrando, A. P. Jardine, W. Allison, J. Ellis, *J. Am. Chem. Soc.* **2008**, *130*, 6789 – 6794.
[14] J. K. Nørskov, N. D. Lang, *Phys. Rev. B* **1980**, *21*, 2131.
[15] H. Hedgeland, P. Fouquet, A. P. Jardine, G. Alexandrowicz, W. Allison, J. Ellis, *Nat. Phys.* **2009**, *5*, 561.
[16] Changes due to the pre-exponential factor are much less important (see the Supporting Information).
[17] C. Uebing, R. Gomer, *Surf. Sci.* **1991**, *259*, 151 – 161.
[18] S. J. Clark, M. D. Segall, C. J. Pickard, P. J. Hasnip, M. J. Probert, K. Refson, M. Payne, *Z. Kristallogr.* **2005**, *220*, 567.
[19] A. Tkatchenko, M. Scheffler, *Phys. Rev. Lett.* **2009**, *102*, 073005.
[20] S. Grimme, *J. Comput. Chem.* **2006**, *27*, 1787.
[21] M. Sacchi, S. Jenkins, H. Hedgeland, A. P. Jardine, B. J. Hinch, *J. Phys. Chem. B* **2011**, *115*, 16134 – 16141.

